



The role of horizontal thermal advection in regulating wintertime mean and extreme temperatures over interior North America during the past and future

Fuyao Wang¹ · Stephen J. Vavrus¹ · Jennifer A. Francis² · Jonathan E. Martin³

Received: 16 January 2019 / Accepted: 27 July 2019
© Springer-Verlag GmbH Germany, part of Springer Nature 2019

Abstract

Horizontal thermal advection plays an especially prominent role in affecting winter climate over continental interiors, where both climatological conditions and extreme weather are strongly regulated by transport of remote air masses. Interior North America is one such region, and it experiences occasional cold-air outbreaks (CAOs) that may be related to amplified Arctic warming. Despite the known importance of dynamics in shaping the winter climate of this sector and the potential for climate change to modify heat transport, limited attention has been paid to the regional impact of thermal advection. Here, we use a reanalysis product and output from the Community Earth System Model's Large Ensemble to quantify the roles of zonal and meridional temperature advection over the central United States during winter, both in the late twentieth and late twenty-first centuries. We frame our findings as a “tug-of-war” between opposing influences of the two advection components and between these dynamical forcings vs. thermodynamic changes under greenhouse warming. During both historical and future periods, zonal temperature advection is stronger than meridional advection east of the Rockies. The model simulates a future weakening of both zonal and meridional temperature advection, such that westerly flow provides less warming and northerly flow less cooling. On the most extreme cold days, meridional cold-air advection is more important than zonal warm-air advection. CAOs in the future feature stronger northerly flow but less extreme temperatures (even relative to the warmer climate), indicating the importance of other mechanisms such as snow cover and sea ice changes.

Keywords Thermal advection · Extreme temperatures · Future projection · CESM large ensemble · North America · Arctic amplification

1 Introduction

Extratropical continental interiors are characterized by high wintertime temperature variability on interannual and intraseasonal timescales (de Vries et al. 2012; Holmes et al. 2016). Low terrestrial heat capacity, episodic snow cover,

and vigorous atmospheric circulation patterns during this season promote large swings in temperature compared with the more moderate fluctuations in mid-latitude oceans. Heat transport by horizontal advection is known to be a major contributor to these thermal variations, yet few studies have quantified the role of thermal advection in affecting the mean wintertime climate of extratropical land masses.

In addition, wintertime extreme temperature events occasionally influence large regions of the populous mid-latitudes. Extreme cold events have attracted widespread attention after a recent series of Cold Air Outbreaks (CAOs) hit the US (Walsh et al. 2001; Cohen et al. 2014; Cellitti et al. 2006; Smith and Sheridan 2018), such as the ones during the winters of 2009/10, 2010/2011, 2013/14 (Wang et al. 2010; Hartmann 2015; Lee et al. 2015; Marinaro et al. 2015; Screen et al. 2015), 2017/18, and 2018/19. All of these CAOs produced significant societal impacts. For example, the early 2014 North American event affected much of

Electronic supplementary material The online version of this article (<https://doi.org/10.1007/s00382-019-04917-8>) contains supplementary material, which is available to authorized users.

✉ Fuyao Wang
fwang26@wisc.edu

¹ Nelson Institute Center for Climatic Research, University of Wisconsin-Madison, Madison, WI 53706, USA

² Woods Hole Research Center, Falmouth, MA, USA

³ Department of Atmospheric and Oceanic Sciences, University of Wisconsin-Madison, Madison, WI, USA

Canada and the United States, resulting in record low temperatures at numerous locations east of the Rockies and leading to the closure of schools and businesses (Screen et al. 2015). Since 2000 over the land area from 20°N to 50°N, the number of icing days and the percentage of cold winter months have been increasing, and the coldest daily minimum temperature is decreasing (Cohen et al. 2014). Using a severe winter weather index, Cohen et al. (2018) conclude that severe CAOs and heavy snowfalls have occurred more frequently in the eastern US during 1990–2016. Extreme warm events during winter receive less attention than CAOs, yet warm spells also have significant ecological and economic impacts. Extreme warmth in late winter causes vegetation to leaf out earlier, but subsequent freezing temperatures can lead to the dieback of young growth (Polgar and Primack 2011). In this paper, both extreme cold and warm events in winter are analyzed.

It is still under debate whether severe winters in middle latitudes can be attributed to enhanced Arctic warming, tropical influences, natural variability, or a combination of some or all of these factors. For example, some studies suggest that prolonged cold spells in mid-latitudes will increase as sea ice loss continues (Honda et al. 2009; Petoukhov and Semenov 2010; Francis and Vavrus 2012; Liu et al. 2012; Tang et al. 2013; Cohen et al. 2018), while others indicate the opposite (Barnes 2013; Barnes et al. 2014; Screen and Simmonds 2013; Screen 2014; Wallace et al. 2014; Screen et al. 2015; Ayarzagüena and Screen 2016). These inconsistencies reflect the likely existence of competing “tug-of-war” effects. The first tug-of-war involves the Arctic and tropics (Barnes and Polvani 2015; Francis 2017). Global warming is amplified in the Arctic (Serreze et al. 2009), where Arctic sea ice is melting dramatically (Vaughan et al. 2013) and the near-surface air temperature is increasing at a pace two-to-three times the global average (Francis 2017; Screen 2017a, b)—a phenomenon known as Arctic Amplification (AA, Serreze et al. 2009; Cohen et al. 2014). It has been suggested that the reduced meridional temperature gradient in the lower troposphere favors a deceleration of midlatitude zonal winds aloft, and possibly a meridional stretching of Rossby waves, which can increase the frequency of blocking events and extreme weather events (Francis and Vavrus 2012). Concurrently, projected global warming is also amplified over the tropical upper troposphere (Barnes and Polvani 2015)—although this warming is larger than the satellite observations and reanalysis indicate (Fu et al. 2011; Seidel et al. 2012; Sohn et al. 2016)—which would strengthen the meridional temperature gradient in upper levels, accelerate the sub-tropical jet stream, and may decrease atmospheric waviness (Vavrus et al. 2017). Although some evidence suggests that AA prevails in this regional tug-of-war and has led to a wavier circulation since the early 1990s (Feldstein and Lee 2014; Francis and Vavrus 2015; Cohen

2016), there is still no clear mechanism for how this dynamic change has affected extreme cold events.

The second tug-of-war competition occurs between dynamic and thermodynamic changes in middle latitudes as the climate warms. The dynamic effect refers to the tendency for AA to promote a more meandering atmospheric circulation and thus stronger northerly winds during winter in some regions, which results in more cold Arctic air transported southward and can produce more extreme cold weather. In contrast, the thermodynamic effect refers to the fact that AA causes northerly winds to transport moderated Arctic air masses southward and thus produce less extreme cold weather. The opposing impacts of the dynamic and thermodynamic influences was noted by Screen (2017a, b), who found that the expected European winter cooling due to a negative North Atlantic Oscillation response to Arctic sea ice loss is canceled by the enhanced upstream warming of the Arctic.

In this paper, we focus on the second tug-of-war. Through investigating the roles of zonal and meridional temperature advection in mean and extreme winter climate conditions over interior North America, both in the recent past (late twentieth century) and the future (late twenty-first century), the thermodynamic and dynamic roles can be decomposed. This study represents the first attempt to systematically quantify the contributions of zonal and meridional temperature advection to mean and extreme winter conditions. The data and methods are introduced in Sect. 2. The observed and simulated recent climatology of horizontal temperature advection are compared in Sect. 3. Future changes in the climatology of horizontal temperature advection are described in Sect. 4, and in Sect. 5, the role of horizontal temperature advection on extreme winter days and its future changes are investigated. The conclusions and further discussion are presented in Sect. 6.

2 Data and methods

2.1 Data

We utilize daily mean data from the European Centre for Medium-Range Weather Forecasts (ECMWF) Re-Analysis Interim (ERA-Interim) dataset with horizontal resolution of $0.7^\circ \times 0.7^\circ$ during the period 1979–2016 (Dee et al. 2011). The results of the ERA-Interim data are used to validate the simulated historical horizontal temperature advection.

To investigate recent horizontal temperature advection and its future changes, we analyze output from the Community Earth System Model Large Ensemble (CESM-LE; Kay et al. 2015). The CESM-LE is a large ensemble run with a fully coupled global model that uses the CESM1 Community Atmospheric Model version 5 (CAM5) as its

atmospheric component. We analyze the simulated historical and projected Representative Concentration Pathway 8.5 (RCP8.5) atmospheric data from 40 realizations of the CESM-LE. Each ensemble member uses observed historical forcing from 1920 to 2005 and RCP8.5 forcing from 2006 to 2100. The ensemble members differ from each other by only small round-off level variations in their atmospheric initial conditions. To compare with the horizontal temperature advection in reanalysis data, the same time period is analyzed by bridging the simulated historical (1979–2005) and projected (2006–2016) outputs together in CESM-LE. To further study the simulated future changes in temperature advection, the late twentieth century (1971–2000) and late twenty-first century (2071–2100) are compared over North America (20°N–75°N, 160°W–50°W). The daily wintertime (December, January, and February) air temperature and zonal and meridional wind fields are used to calculate horizontal temperature advection at 850 hPa, which is the only lower-tropospheric level in CESM-LE where the required daily output was saved.

2.2 The climatology of horizontal temperature advection

The horizontal temperature advection includes two parts: zonal ($-U \frac{\partial T}{\partial x}$) and meridional ($-V \frac{\partial T}{\partial y}$) temperature advection, where T , U , and V represent air temperature, zonal, and meridional wind, respectively. The common time period 1979–2016 is analyzed when comparing the reanalysis and simulated horizontal temperature advection climatology, although the horizontal temperature advection during this period and 1970–2000 is almost the same. To indicate the time period, the subscripts “his” or “rcp” are added. For example, $-U_{his} \frac{\partial T_{his}}{\partial x}$ and $-V_{rcp} \frac{\partial T_{rcp}}{\partial y}$ represent historical zonal temperature advection and projected meridional temperature advection, respectively.

The climatology of horizontal temperature advection (*termA*) in each time period is represented with an overbar. For instance, $\overline{-U_{his} \frac{\partial T_{his}}{\partial x}}$ and $\overline{-V_{rcp} \frac{\partial T_{rcp}}{\partial y}}$ represent the climatology of historical zonal temperature advection and the climatology of projected meridional temperature advection, respectively. The climatology of temperature advection (*termA*) can be further broken down into two terms by decomposing each variable into its climatology ($\bar{\quad}$) and the anomaly from its climatology (\prime):

$$T_{his} = \overline{T_{his}} + T'_{his} \tag{1}$$

$$U_{his} = \overline{U_{his}} + U'_{his} \tag{2}$$

Substituting (1) and (2) into $\overline{-U_{his} \frac{\partial T_{his}}{\partial x}}$ yields:

$$\begin{aligned} \overline{-U_{his} \frac{\partial T_{his}}{\partial x}} &= \overline{-\left(\overline{U_{his}} + U'_{his}\right) \frac{\partial \left(\overline{T_{his}} + T'_{his}\right)}{\partial x}} \\ &= \overline{-U_{his} \frac{\partial T_{his}}{\partial x}} - \overline{U'_{his} \frac{\partial T_{his}}{\partial x}} - \overline{\overline{U_{his}} \frac{\partial T'_{his}}{\partial x}} - \overline{U'_{his} \frac{\partial T'_{his}}{\partial x}} \\ &= \overline{-U_{his} \frac{\partial T_{his}}{\partial x}} - \overline{U'_{his} \frac{\partial T_{his}}{\partial x}} - \overline{\overline{U_{his}} \frac{\partial T'_{his}}{\partial x}} - \overline{U'_{his} \frac{\partial T'_{his}}{\partial x}} \end{aligned} \tag{3}$$

Because $\overline{T'_{his}}$ and $\overline{U'_{his}}$ are equal to 0, the last 2 terms on the right-hand-side (RHS) of (3) are also 0.

The same decomposition of historical meridional temperature advection and projected zonal and meridional advection creates the following set of equations (Eqs.):

$$\left\{ \begin{aligned} \overline{-U_{his} \frac{\partial T_{his}}{\partial x}} &= \overline{-U_{his} \frac{\partial T_{his}}{\partial x}} + \overline{-U'_{his} \frac{\partial T'_{his}}{\partial x}} \\ \overline{-V_{his} \frac{\partial T_{his}}{\partial y}} &= \overline{-V_{his} \frac{\partial T_{his}}{\partial y}} + \overline{-V'_{his} \frac{\partial T'_{his}}{\partial y}} \\ \overline{-U_{rcp} \frac{\partial T_{rcp}}{\partial x}} &= \overline{-U_{rcp} \frac{\partial T_{rcp}}{\partial x}} + \overline{-U'_{rcp} \frac{\partial T'_{rcp}}{\partial x}} \\ \overline{-V_{rcp} \frac{\partial T_{rcp}}{\partial y}} &= \overline{-V_{rcp} \frac{\partial T_{rcp}}{\partial y}} + \overline{-V'_{rcp} \frac{\partial T'_{rcp}}{\partial y}} \end{aligned} \right. \tag{4}$$

termA = termB + termC

We call the first term (*termB*) on the RHS of Eq. (4) the pure climatology term, since it represents advection of the climatological temperature gradient by the climatological wind. The second term (*termC*) is the nonlinear term, which represents advection of the anomalous temperature gradient by the anomalous wind relative to its climatology.

2.3 The change in horizontal temperature advection

The change of horizontal temperature advection between the late twenty-first and late twentieth centuries (*diffA*) is defined as $\text{termA}_{rcp} - \text{termA}_{his}$. Then,

$$\left\{ \begin{aligned} \left\{ -\overline{U_{rcp}} \frac{\partial T_{rcp}}{\partial x} - \left(-\overline{U_{his}} \frac{\partial T_{his}}{\partial x} \right) \right\} &= \left\{ -\Delta U \frac{\partial \overline{T_{his}}}{\partial x} \right\} + \left\{ -\overline{U_{his}} \frac{\partial \Delta T}{\partial x} \right\} + \left\{ -\Delta U \frac{\partial \Delta T}{\partial x} \right\} + \left\{ -\overline{U'_{rcp}} \frac{\partial T'_{rcp}}{\partial x} - \left(-\overline{U'_{his}} \frac{\partial T'_{his}}{\partial x} \right) \right\} \\ \left\{ -\overline{V_{rcp}} \frac{\partial T_{rcp}}{\partial y} - \left(-\overline{V_{his}} \frac{\partial T_{his}}{\partial y} \right) \right\} &= \left\{ -\Delta V \frac{\partial \overline{T_{his}}}{\partial y} \right\} + \left\{ -\overline{V_{his}} \frac{\partial \Delta T}{\partial y} \right\} + \left\{ -\Delta V \frac{\partial \Delta T}{\partial y} \right\} + \left\{ -\overline{V'_{rcp}} \frac{\partial T'_{rcp}}{\partial y} - \left(-\overline{V'_{his}} \frac{\partial T'_{his}}{\partial y} \right) \right\} \end{aligned} \right. \quad \text{diffA} = \text{diffB1} + \text{diffB2} + \text{diffB3} + \text{diffC} \quad (5)$$

where, $\Delta U = \overline{U_{rcp}} - \overline{U_{his}}$, $\Delta V = \overline{V_{rcp}} - \overline{V_{his}}$, and $\Delta T = \overline{T_{rcp}} - \overline{T_{his}}$.

We call the first three terms on the RHS of Eq. (5) the dynamic term (*diffB1*), thermodynamic term (*diffB2*), and higher-order term (*diffB3*), and the sum of the last 2 terms the nonlinear term (*diffC*). The dynamic term (*diffB1*) represents the temperature advection change caused by a change in wind. The thermodynamic term (*diffB2*) represents the temperature advection change caused by a change in the temperature gradient. The higher-order term (*diffB3*) indicates the temperature advection change caused by both a change in wind and temperature gradient, which is usually one order of magnitude smaller than *diffB1* and *diffB2*. The sum of *diffB1*, *diffB2* and *diffB3* equals $\text{termB}_{rcp} - \text{termB}_{his}$.

To measure the importance of each component to the total change of advection, the percentage contribution from each term is calculated by dividing *diffA* on both sides of Eq. (5),

$$1 = \frac{\text{diffB1}}{\text{diffA}} + \frac{\text{diffB2}}{\text{diffA}} + \frac{\text{diffB3}}{\text{diffA}} + \frac{\text{diffC}}{\text{diffA}} \quad (6)$$

2.4 The change in horizontal temperature advection on extreme days

Our analysis of extreme days targets the central US (CUS: 30°N–50°N, 100°W–85°W), a relatively homogeneous region that avoids topographic complications (Fig. S1), exhibits large wintertime temperature variability (Fig. S2), and has experienced many CAOs (Walsh et al. 2001; Vavrus et al. 2017). We sort the area-averaged CUS 2-m daily air temperature (*T2m*) during winter into 20 bins, ranging from the coldest to warmest 5% of all days. Extreme days are defined here as the 5% coldest and 5% warmest days in the historical and future time periods. For each bin there are 5400 cases (30years × 90winter days × 40ensemble members × 5%).

The climatology of zonal temperature advection can therefore be written as:

$$-\overline{U_{his}} \frac{\partial \overline{T_{his}}}{\partial x} = \sum_{i=1}^{nbin} \left[-\overline{U_{his}} \frac{\partial \overline{T_{his}}}{\partial x} \right]_i \quad (7)$$

where *i* indicates the bin number, and *nbin* is the total number of bins (20). $[\]_i$ indicates the mean over the *i*th bin. For each bin the horizontal temperature advection can be decomposed into four terms:

$$\left\{ \begin{aligned} \left[-\overline{U_{his}} \frac{\partial \overline{T_{his}}}{\partial x} \right]_i &= \left\{ -\overline{U_{his}} \frac{\partial \overline{T_{his}}}{\partial x} \right\} + \left[-\overline{U'_{his}} \frac{\partial \overline{T_{his}}}{\partial x} \right]_i + \left[-\overline{U_{his}} \frac{\partial T'_{his}}{\partial x} \right]_i + \left[-\overline{U'_{his}} \frac{\partial T'_{his}}{\partial x} \right]_i \\ \left[-\overline{V_{his}} \frac{\partial \overline{T_{his}}}{\partial y} \right]_i &= \left\{ -\overline{V_{his}} \frac{\partial \overline{T_{his}}}{\partial y} \right\} + \left[-\overline{V'_{his}} \frac{\partial \overline{T_{his}}}{\partial y} \right]_i + \left[-\overline{V_{his}} \frac{\partial T'_{his}}{\partial y} \right]_i + \left[-\overline{V'_{his}} \frac{\partial T'_{his}}{\partial y} \right]_i \\ \left[-\overline{U_{rcp}} \frac{\partial \overline{T_{rcp}}}{\partial x} \right]_i &= \left\{ -\overline{U_{rcp}} \frac{\partial \overline{T_{rcp}}}{\partial x} \right\} + \left[-\overline{U'_{rcp}} \frac{\partial \overline{T_{rcp}}}{\partial x} \right]_i + \left[-\overline{U_{rcp}} \frac{\partial T'_{rcp}}{\partial x} \right]_i + \left[-\overline{U'_{rcp}} \frac{\partial T'_{rcp}}{\partial x} \right]_i \\ \left[-\overline{V_{rcp}} \frac{\partial \overline{T_{rcp}}}{\partial y} \right]_i &= \left\{ -\overline{V_{rcp}} \frac{\partial \overline{T_{rcp}}}{\partial y} \right\} + \left[-\overline{V'_{rcp}} \frac{\partial \overline{T_{rcp}}}{\partial y} \right]_i + \left[-\overline{V_{rcp}} \frac{\partial T'_{rcp}}{\partial y} \right]_i + \left[-\overline{V'_{rcp}} \frac{\partial T'_{rcp}}{\partial y} \right]_i \end{aligned} \right. \quad \text{termA}_i = \text{termB} + \text{termD}_i + \text{termE}_i + \text{termC}_i \quad (8)$$

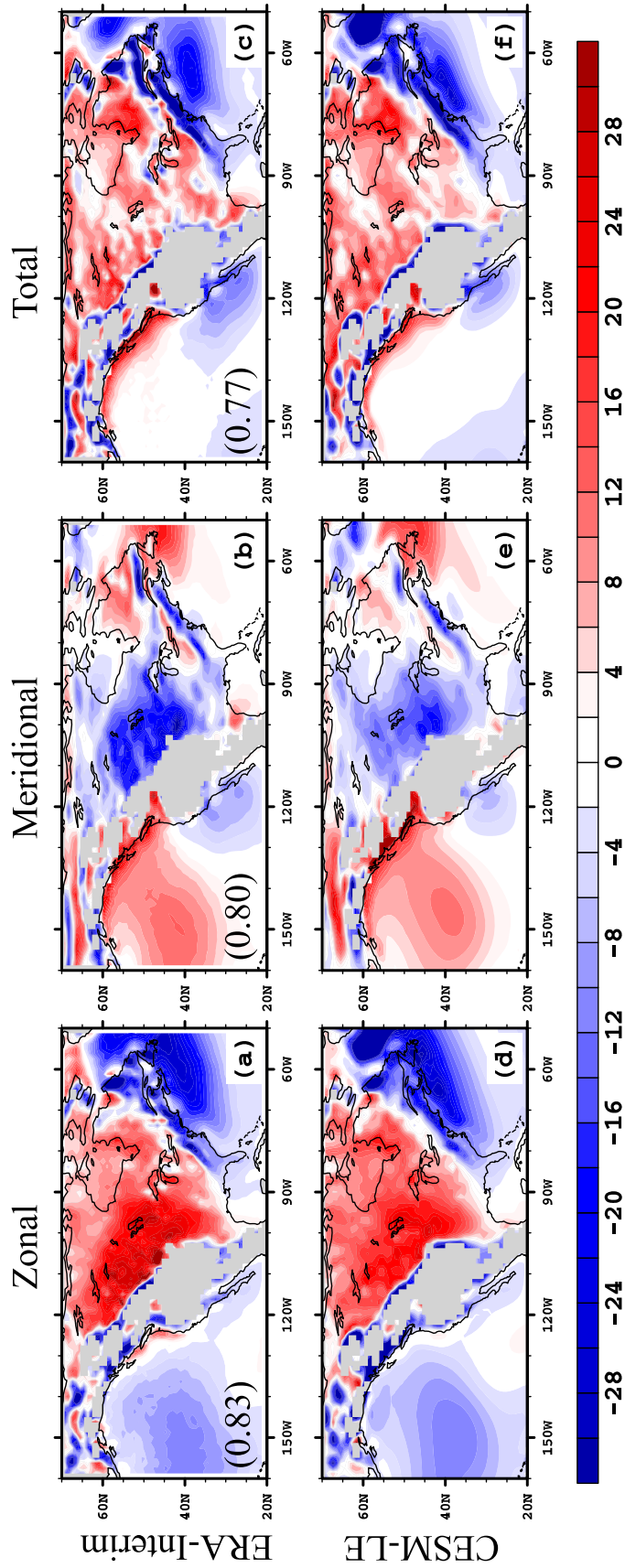


Fig. 1 Climatology of wintertime (DJF) zonal (a, d), meridional (b, e), and total (zonal + meridional, c, f) horizontal temperature advection (units: K/year) at 850 hPa using daily outputs of ERA-Interim (a–c) and CESM-LE historical experiment (d–f) during 1979–2016. The numbers on a–c indicate the spatial correlation of zonal, meridional, and total horizontal temperature advection between ERA-Interim and CESM-LE over North America, respectively. Area higher than 1500 m is masked

For each bin, the temperature advection consists of the pure climatology term ($termB$), which is the same $termB$ as in Eq. (4), the temperature advection of the climatological temperature gradient by wind anomalies in the bin ($termD_i$), the temperature advection of anomalous temperature gradient in the bin by the climatological wind ($termE_i$), and the nonlinear term in the bin ($termC_i$). The average of all the bins in Eq. (8) equals the corresponding terms in Eq. (4):

$$\begin{aligned} \sum_{i=1}^{nbin} termA_i &= termA \\ \sum_{i=1}^{nbin} termC_i &= termC \\ \sum_{i=1}^{nbin} termD_i &= \sum_{i=1}^{nbin} termE_i = 0 \end{aligned} \quad (9)$$

A student t-test is applied to determine significant changes (p value < 0.05) in each grid point. The difference

in the seasonal average of all 40 ensemble members between the historical and projected periods is first calculated. The t-value is then determined, based on the variance among ensemble members within each of the two time periods. The same procedure is applied for extreme days, except that the means and variances on extreme days are used. For the wind fields, if either the zonal or meridional wind component change is significant, then the future wind velocity is considered to be significantly different from the historical period.

3 The observed and simulated climatology of horizontal temperature advection

In this section, the climatology of the total zonal and meridional temperature advection ($termA$) and its two components—pure climatology term ($termB$) and nonlinear term ($termC$)—from Eq. (4) are compared between CESM-LE and ERA-Interim.

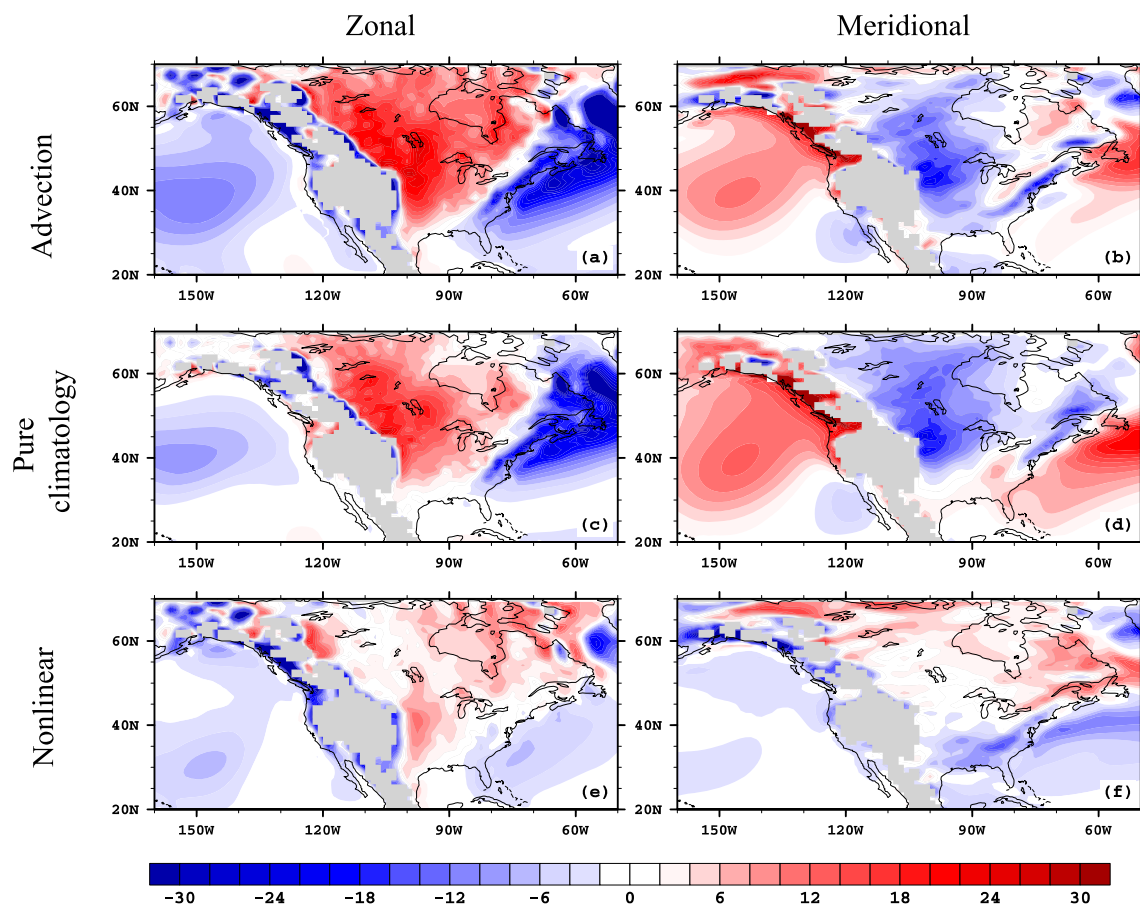


Fig. 2 Climatology of wintertime (DJF) total zonal and meridional temperature advection (a, b; $termA$ in equation set 4) and their two components: the pure climatology term (c, d; $termB$ in equation set

4) and nonlinear term (e, f; $termC$ in equation set 4) in CESM-LE (unit: K/year) during the late twentieth century (1971–2000). Area higher than 1500 m is masked

During winter, ERA-Interim indicates that the lower-level (850 hPa) mean zonal temperature advection warms the air between the Rocky Mountains and the Appalachian Mountains (Fig. 1a), while mean meridional temperature advection cools it (Fig. 1b). Zonal and meridional temperature advection thus oppose each other, but the zonal component is a bit stronger, such that the total effect is a modest but widespread warming over the interior of North America (Fig. 1c). The simulated zonal, meridional, and total temperature advection climatology in CESM-LE (Fig. 1d–f) largely reproduces the patterns of ERA-Interim (Fig. 1a–c). Spatial correlations of zonal, meridional, and total advection between CESM-LE and ERA-Interim over North America are high (0.83, 0.80, and 0.77, respectively). During winter, the lower-level atmosphere is generally warmer over oceans than over land, and the majority of North America experiences westerly winds on average. Thus, mild Pacific air is carried eastward over the Rockies, where it is further warmed by compression on the leeward side, and then warms the interior of North America. In regions near the Rockies (e.g., the Mackenzie River Basin), the amount of downslope adiabatic heating is comparable to the magnitude of horizontal advection (Szeto 2008). The strong downslope winds occurring in the lee-side of the Rockies are generally a local phenomenon, which do not extend to the Plains (Brinkmann 1974). The decreased warming from the Rockies to the east also indicates a weakening adiabatic heating effect, but determining the relative contributions of adiabatic heating and land-sea temperature contrast is beyond the scope of this study. Meanwhile, since the Arctic is generally colder than middle latitudes, the prevailing northerly winds bring cold Arctic air southward into the CUS, causing meridional temperature advection to cool the area to the east of the Rockies. Both components cool the East Coast.

To investigate the strength of dynamic and thermodynamic terms in the “tug-of-war”, we decompose the total zonal and meridional temperature advection term ($termA$) in both ERA-Interim (not shown) and CESM-LE into two terms: the pure climatology term ($termB$, Fig. 2c, d) and the nonlinear term ($termC$, Fig. 2e, f), as shown in Eqs. (4). The CESM-LE can also reproduce the spatial pattern of the two components of the total zonal and meridional temperature advection, with spatial correlation 0.83 (zonal) and 0.89 (meridional) for the pure climatology terms and 0.79 (zonal) and 0.81 (meridional) for the nonlinear terms, compared with ERA-Interim. Thus, the CESM-LE output is deemed suitable to investigate the role of horizontal temperature advection in regulating wintertime climate and extreme events over North America. From this point forward, only CESM-LE results are shown.

The spatial pattern of mean zonal temperature advection (Fig. 2a) is dominated by the pure climatology term (Fig. 2c), with a spatial correlation of 0.87 over North

America. During winter, prevailing westerly winds affect most of the North American continent (Fig. 3c), and the spatial pattern of the pure climatology term of zonal temperature advection is determined by the zonal temperature gradient (Fig. 3g). The sign of the nonlinear term is generally consistent with the total zonal temperature advection, but with a considerably smaller magnitude (Fig. 2e).

The spatial pattern of meridional temperature advection climatology (Fig. 2b) is also dominated by the pure climatology term (Fig. 2d), with a spatial correlation of 0.75 over North America. The pure climatology term is determined mainly by the mean meridional wind (Fig. 3e), which is southerly over the Pacific region, northerly over the central continent, and southerly to the east of the North America, corresponding to the mean ridge–trough–ridge geopotential height distribution. Because the temperature distribution features cold air to the north and warm air to the south, the meridional temperature gradient is negative everywhere except near the mountain region (Fig. 3i). Therefore, the pure climatology term warms the North Pacific Ocean by transporting warm air from low latitudes and cools the North American continent by bringing cold Arctic air southward.

4 Future changes in horizontal temperature advection from CESM-LE

The change in temperature advection ($diffA$) can be represented by the change in the pure climatology term ($diffB$) plus the change in the nonlinear term ($diffC$). As shown in Eq. (5), the change in $diffB$ can be further decomposed into a dynamic term ($diffB1$), thermodynamic term ($diffB2$), and higher-order term ($diffB3$) to quantify the contribution of dynamic and thermodynamic changes.

Under the influence of increasing greenhouse gas concentrations, the air temperature increases everywhere but not uniformly, such that air over land generally warms more than air over adjacent oceans, and high latitudes warm more than low latitudes (Fig. 3b). Therefore, the change in zonal temperature gradient is positive to the east of the Rockies (Fig. 3h), i.e. less zonal temperature contrast, while the meridional temperature gradient weakens over northern North America (Fig. 3j). The future change in zonal wind consists of a weaker wind to the north and stronger wind to the south (Fig. 3d). Over North America east of the Rockies, the zonal wind weakens nearly everywhere (Fig. 3d). The northerly wind weakens (less northerly flow) along the east side of the Rockies and slightly strengthens (more northerly flow) or changes little in much of eastern North America (Fig. 3f).

In the future, zonal temperature advection decreases over land across central Canada (Fig. 4a), indicating that it warms the land less compared to the historical period. Among all

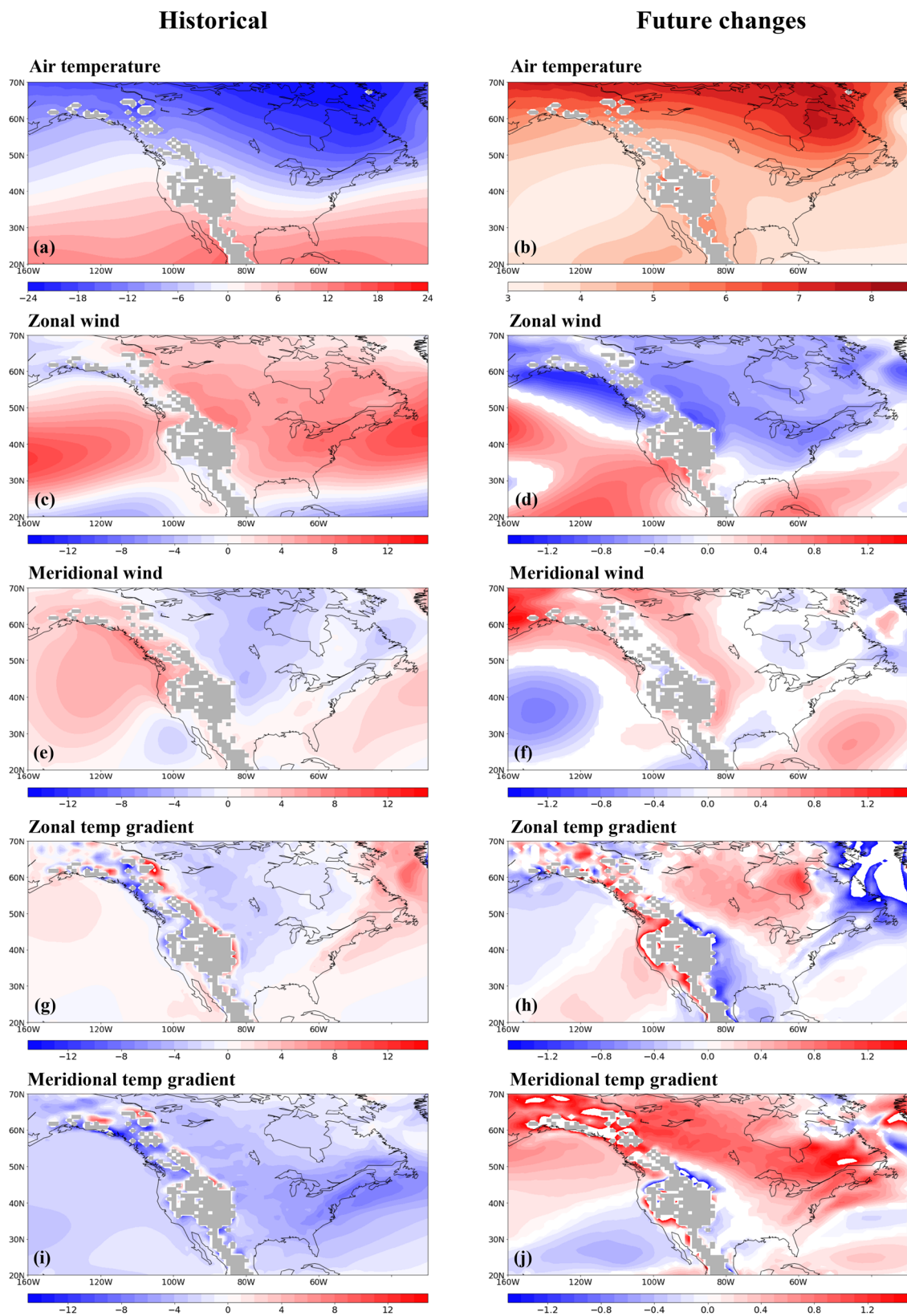


Fig. 3 Historical climatology (1971–2000) and future changes (2071–2100 vs 1971–2000) in 850 hPa **a, b** air temperature ($^{\circ}\text{C}$), **c, d** zonal wind (m/s), **e, f** meridional wind (m/s), **g, h** zonal temperature gradient ($3 \times 10^7 \text{ Km}^{-1}$), and **i, j** meridional temperature gradient

($3 \times 10^7 \text{ Km}^{-1}$). Area higher than 1500 m is masked. Only differences which are significant at the 95% confidence level from a Student's t-test are shown

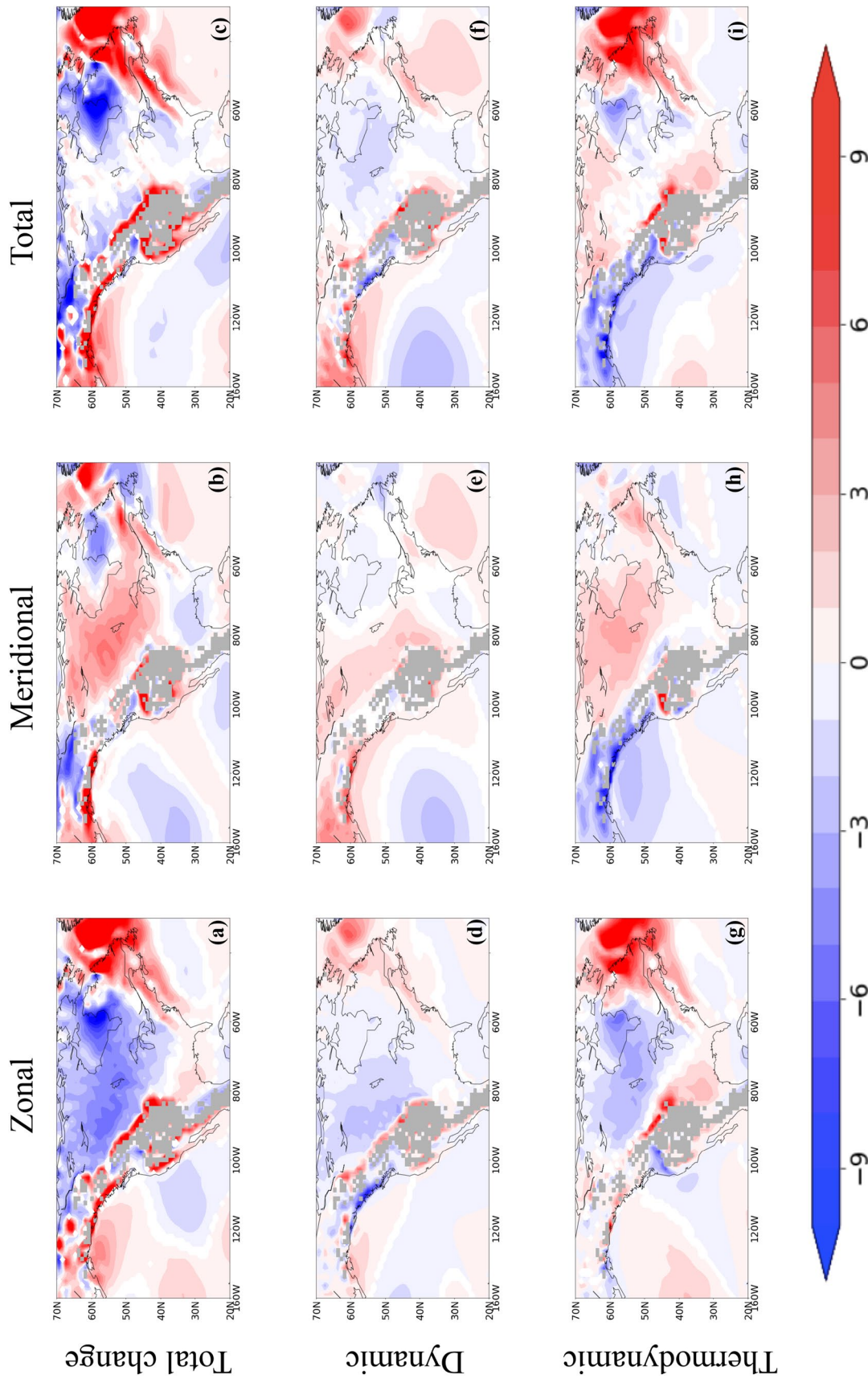
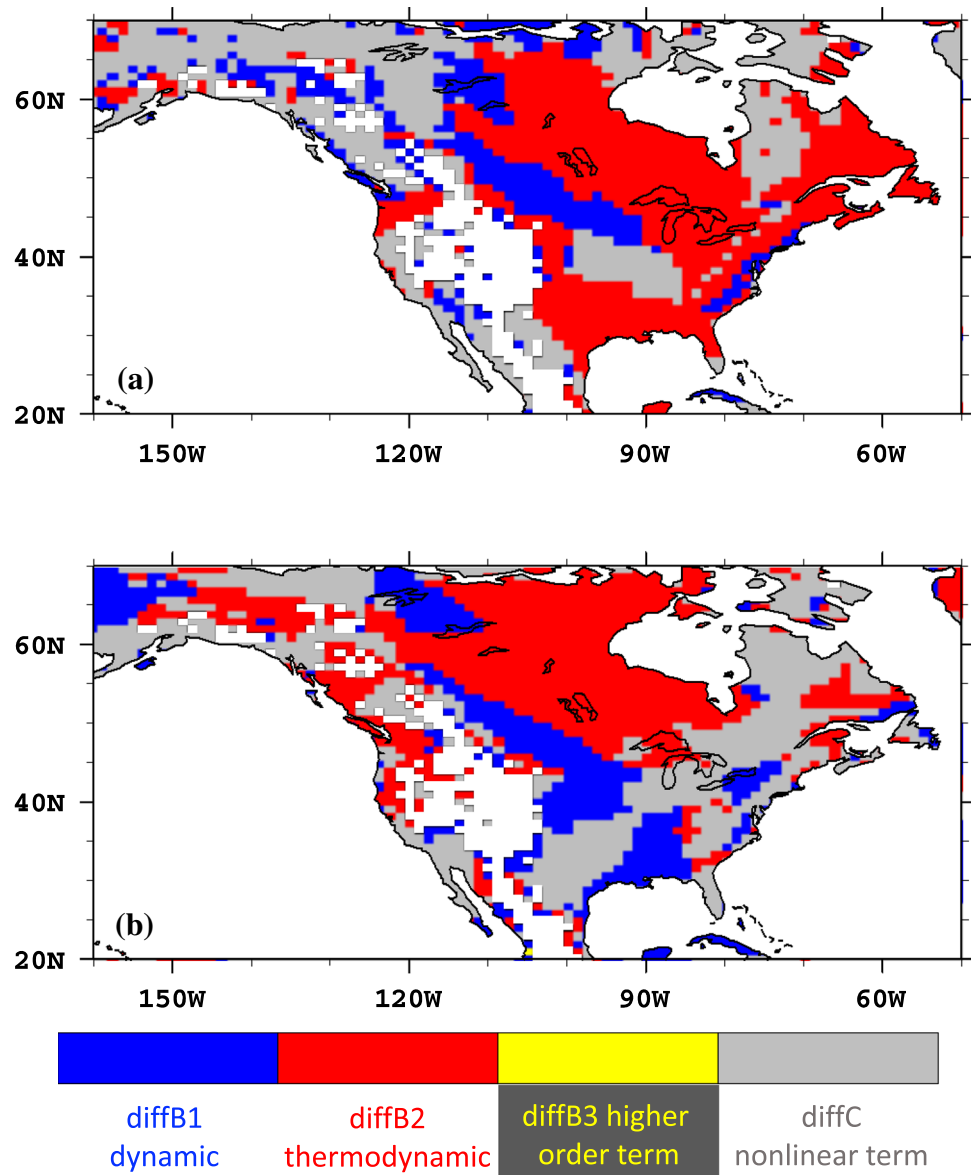


Fig. 4 Future changes (2071–2100 vs 1971–2000) in 850 hPa horizontal temperature advection and its components in CESM-LE (unit: K/year). Total change (*dif*), dynamic term (*difB1*), and thermodynamic (*difB2*) are shown in **a–c**, **d–f**, and **g–i**, respectively. The zonal, meridional and total advection are shown in **(a, d, g)**, **(b, e, h)**, and **(c, f, i)**, respectively. Area higher than 1500 m is masked. Only differences which are significant at the 95% confidence level from a Student's t-test are shown

Fig. 5 The most important term for future changes in **a** zonal and **b** meridional temperature advection at each grid point. Area higher than 1500 m is masked



its components, the thermodynamic term contributes the most (Fig. 4g), indicating that the advection does not warm the land as effectively as before, due to the weakened zonal temperature gradient. The dynamic term also has some contribution to the total advection change, but its main impact is limited to the west side of central Canada (Fig. 4d). That is due to the weakened westerly wind there, which transports less warm air over the continental interior (Fig. 3d). Both thermodynamic and dynamic terms change in the same direction and act to cool most of central North America east of the Rockies (Fig. 4d, g), while the East Coast tends to be warmed. To illustrate which term is most important across the domain, we use Eq. (6) to compute the percentage that each term contributes to zonal and meridional advection, and color each grid point by the term that makes the largest contribution (Fig. 5). It is obvious that in the interior of

North America, the thermodynamic and dynamic terms are the two most important contributors in both the zonal and meridional directions, although the nonlinear term is dominant in some places, especially for meridional advection.

The meridional temperature advection becomes less negative over central Canada, indicating it cools the land less in the future (Fig. 4b). The thermodynamic term dominates the anomalous warming over central Canada (Figs. 4h, 5b), indicating that although the mean northerly wind still brings cold Arctic air southward in the future, Arctic air masses become warmer, and thus northerly winds across central Canada transport milder Arctic air southward and cool the land less. By contrast, the dynamic term changes mainly along the east side of the Rockies (Fig. 4e), where the northerly wind weakens in the future (Fig. 3f) and brings less cold Arctic air southward. The dynamic and thermodynamic

terms change in the same direction, such that both of them tend to further warm the area to the east of the Rockies in the future.

In summary, during the historical period, zonal temperature advection warms most of North America east of the Rockies, while meridional temperature advection cools this region by transporting cold Arctic air southward, such that the net effect is a slight warming. In the future, both zonal and meridional temperature advection weaken over this region, meaning that zonal (meridional) temperature advection warms (cools) the land less. For both zonal and meridional advection changes, the thermodynamic term is generally the most important (Fig. 5), while the higher-order and nonlinear terms (Figures not shown) are generally smaller than the dynamic and thermodynamic terms. For both zonal and meridional temperature advection, the dynamic and thermodynamic terms generally change the same direction. The net change in zonal plus meridional change is only slightly negative over most of the interior of North America (Fig. 4c), indicating the changes of zonal and meridional temperature advection nearly offset each other.

5 Mean horizontal temperature advection and its future changes on extreme days

The role of horizontal advection and its terms on extreme winter days (5% coldest and 5% warmest, Fig. 6) are further investigated in this section. Before investigating the projected advection terms, the simulated historical terms are compared with reanalysis. The simulated terms on extreme days (Figs. 7 and 8) largely reproduce those in ERA-Interim reanalysis data (Fig. S3 and S4). To avoid the confounding influence of general future warming, extreme days are identified relative to the climate in each time period, following Ayarzagüena and Screen (2016), such that both the historical and future 30-year periods contain the same number of extreme days.

The target study region for extreme events is the CUS (Fig. S1), due to its large temperature variability and occasional CAOs (Walsh et al. 2001; Cellitti et al. 2006; Gao et al. 2015; Cohen et al. 2018). To put extreme cold and warm days into context, the T2 m departures of each bin from the historical climatology are shown in Fig. 6, with temperature anomalies systematically changing from negative to positive. The cold or warm anomalies peak in the targeted CUS region and decay gradually to the surroundings. The corresponding spatial patterns for the future (2071–2100) look similar (not shown).

On the extreme cold days, almost the entire continental interior is enveloped by extremely cold air (Fig. 6a), and meridional temperature advection plays a vital role in cooling the CUS (Fig. 7b), while the zonal temperature advection

generally warms this region (Fig. 7a). These advection components on extreme cold days ($termA_1$, Fig. 7a, b) can be further decomposed into four terms: dynamic term ($termD_1$, Fig. 7c, d), thermodynamic term ($termE_1$, Fig. 7e, f), nonlinear term ($termC_1$, Fig. 7g, h), and pure climatology term ($termB$, Fig. 2c, d). Since the pure climatology term is the same across all the bins, it does not help distinguish extreme cold and warm days, so we only focus on the other three terms. Among these, the meridional dynamic term (Fig. 7d) contributes the most to extreme cold over the CUS because on these days, the atmospheric circulation is anomalously wavy and thus the northerly wind component strengthens over the CUS (Fig. 9). This stronger wind flow brings Arctic air masses as far south as the Gulf of Mexico, such that the dynamic term cools a large region from central Canada to southeastern North America (Fig. 7d). Meanwhile, the weakened westerly wind on extreme cold days (Figure not shown) brings less warm air eastward, causing the zonal dynamic term to also cool the area but much less strongly (Fig. 7c). The second most important cooling influence is from the meridional nonlinear term, especially over the southeast US (Fig. 7h), due to the combination of a strengthened northerly wind and an enhanced meridional temperature gradient over the southeast US when a polar air mass is directly upwind.

On extremely warm winter days in the CUS during the historical period, very warm air covers the eastern two-thirds of the continent (Fig. 6t). In contrast to extreme cold days, when zonal and meridional temperature advection oppose each other, these two advection components work together to generally warm the CUS on the warmest days (Fig. 8a, b). The meridional component contributes most, while the zonal component mainly stems from the pure climatology term (Fig. 2c), which is the same across all bins. The meridional dynamic term ($termD_{20}$, Fig. 8d) is the most important on extremely warm days, due to a strong southerly wind transporting warm air from the Gulf of Mexico (Fig. 9e).

In the future simulation, the coldest days are not as bitter as in the recent climate (Fig. 10a, d), even relative to the warmer mean climate, with one warming center over Hudson Bay and one to the southwest of the Great Lakes (Fig. 10g). The warming effect around and downstream of the Great Lakes comes mainly from the meridional nonlinear term (Fig. 12k) and zonal and meridional thermodynamic terms (Fig. 12g, h). The enhanced northerly flow over the CUS (Fig. 10i) causes the meridional dynamic term, which plays a vital role in generating extreme cold days, to become stronger and to cool the region even more (Fig. 12e). This cooling effect, however, is largely offset by the warming effect from the thermodynamic term (Fig. 12h). Overall, the total change in horizontal advection on extremely cold days over the CUS is minimal (Fig. 12c) and therefore cannot explain the temperature moderation over this region in the future. An alternative factor is the impact of future

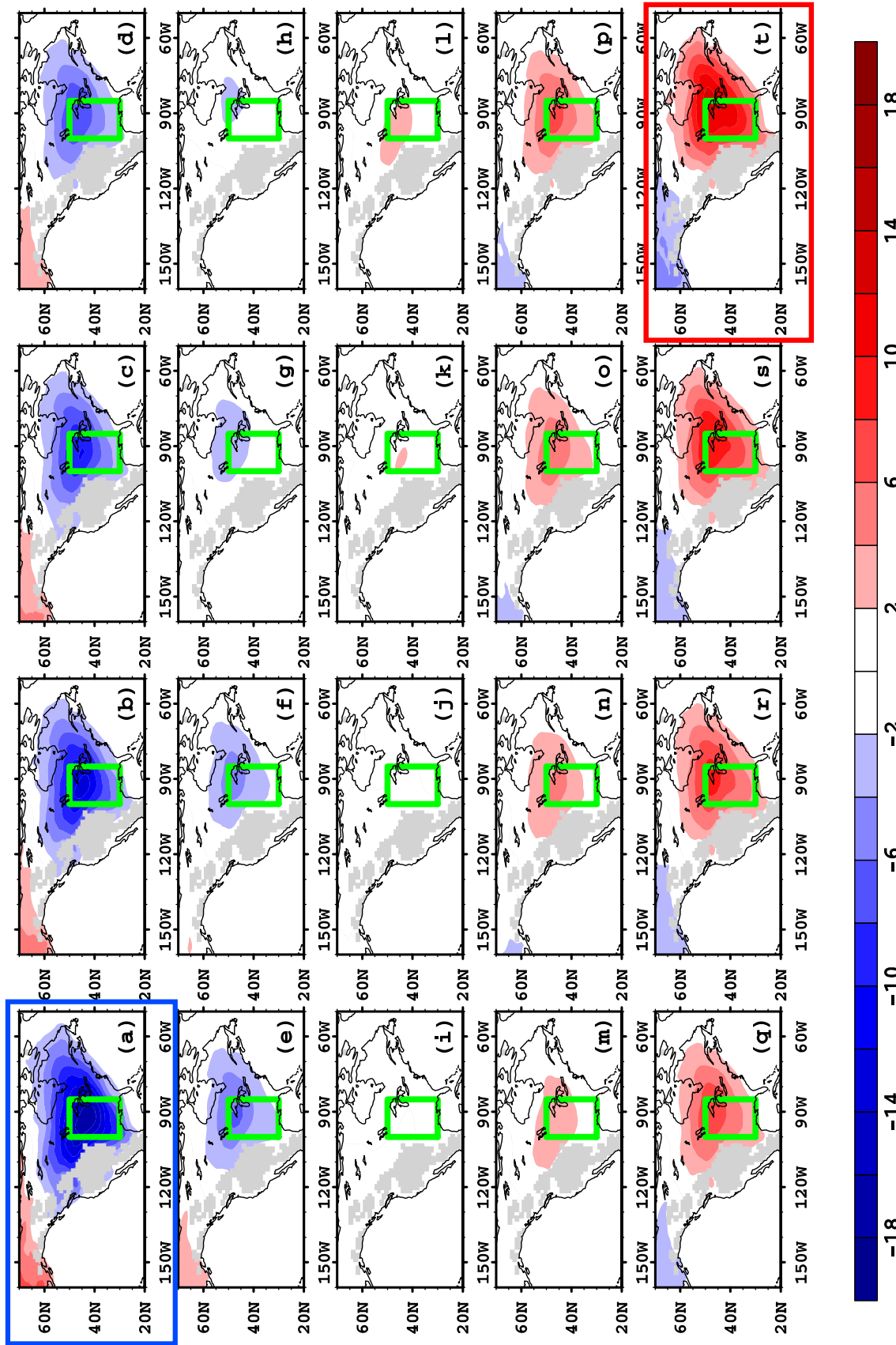


Fig. 6 Wintertime 2-m air temperature anomalies (K) simulated by CESM-LE in the late twentieth century (1971–2000) among 20 bins area-averaged over the central US (green box), ranging from the 5th percentile (upper left) to the 95th percentile (lower right). Area higher than 1500 m is masked. The extreme cold (blue box) and warm days (red box) are highlighted

5% coldest days

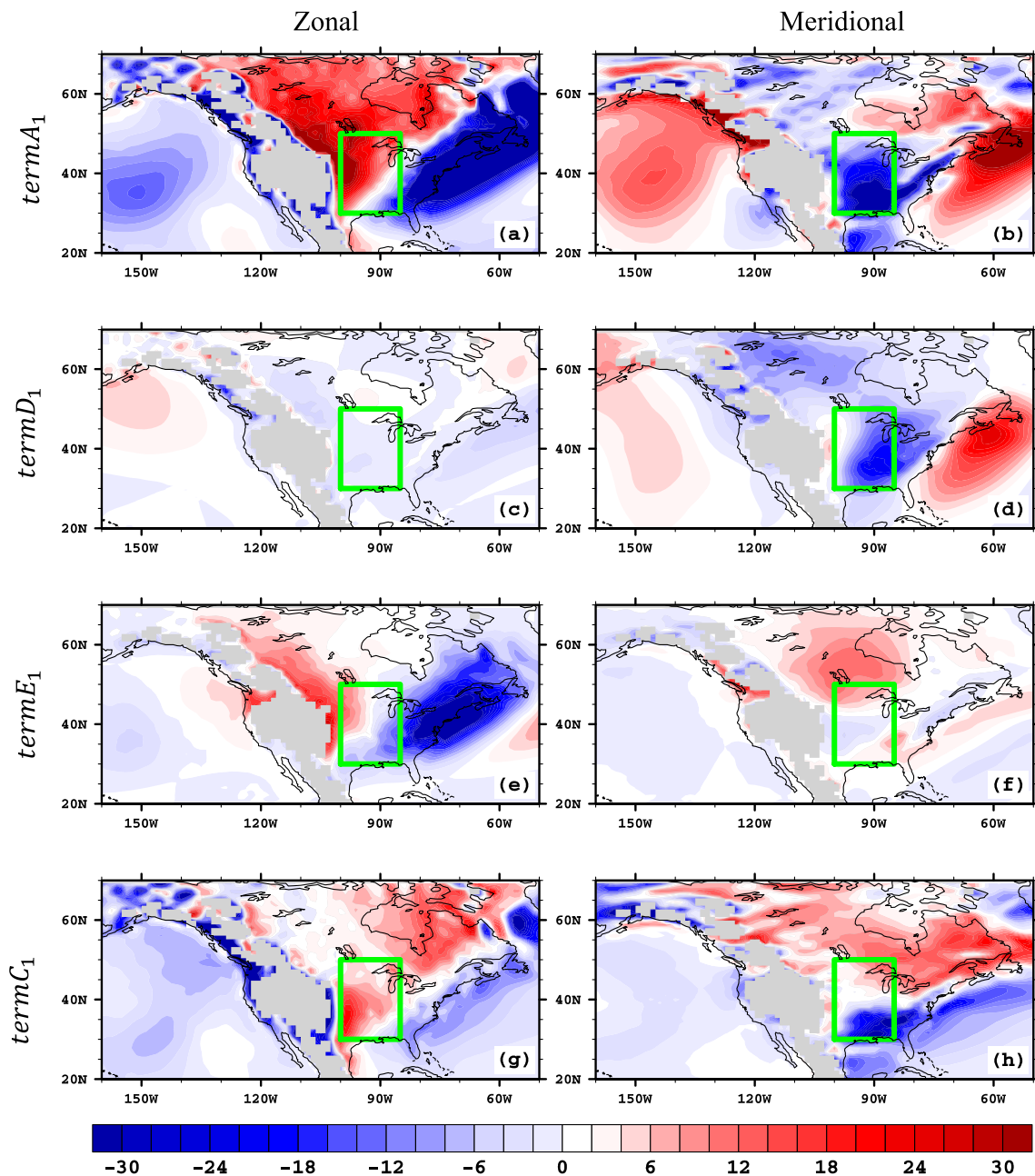


Fig. 7 Temperature advection and its components on extreme CUS wintertime cold days during late twentieth century (1971–2000) in CESM-LE (unit: K/year). Zonal (a, c, e, g) and meridional (b, d, f, h) temperature advection (a, b, $termA_1$ in Eq. 8) and their components:

dynamic term (c, d, $termD_1$ in Eq. 8), thermodynamic term (e–f, $termE_1$ in Eq. 8), and nonlinear term (g, h, $termC_1$ in Eq. 8). Area higher than 1500 m is masked

reductions in snow cover and sea ice on the atmosphere (Vavrus 2007; Gao et al. 2015). The projected snow cover fraction significantly decreases on extreme cold days over mid-latitude North America as the snow margin retreats northward (Fig. 13b). The much lower albedo and lower insulation capacity of bare land versus snow cover helps the

land surface warm more in the future, consistent with the weakened troughing anomaly over interior North America on the coldest days (Fig. 10h). Likewise, the shrinking sea ice cover in Hudson Bay (Fig. 13a; Hochheim and Barber 2014) corresponds to the warming center directly above it (Fig. 10g). On the warmest days, in contrast, neither the

5% warmest days

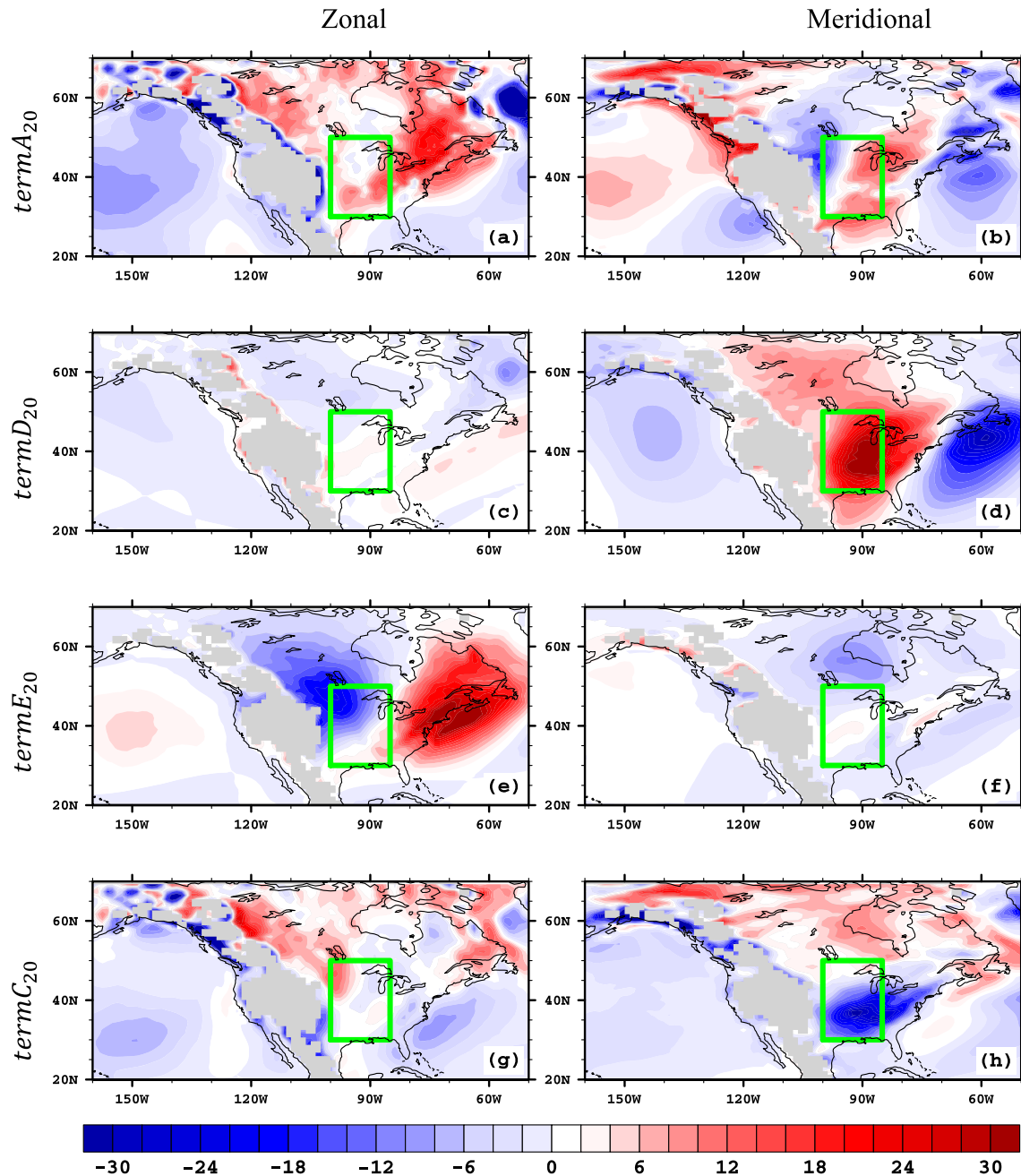


Fig. 8 Same as Fig. 7 but for the 5% warmest winter days

temperature anomalies nor the atmosphere circulation changes as much in the future as on the coldest days over the CUS (Fig. 11g–i).

In summary, on extreme cold and warm days in the CUS, the meridional dynamic term ($termD_i$) is the most important (Figs. 7d, 8d). In the future, air temperature anomalies on the coldest days change more (weaken) than they do on

the warmest days (Figs. 10g, 11g). Another “tug-of-war” therefore appears to exist on extreme cold days in the future between enhanced dynamic advection aloft favoring more cooling and surface-based thermal forcing from reduced snow and sea ice cover favoring warmer Arctic air masses that result in less severe cooling in the CUS.

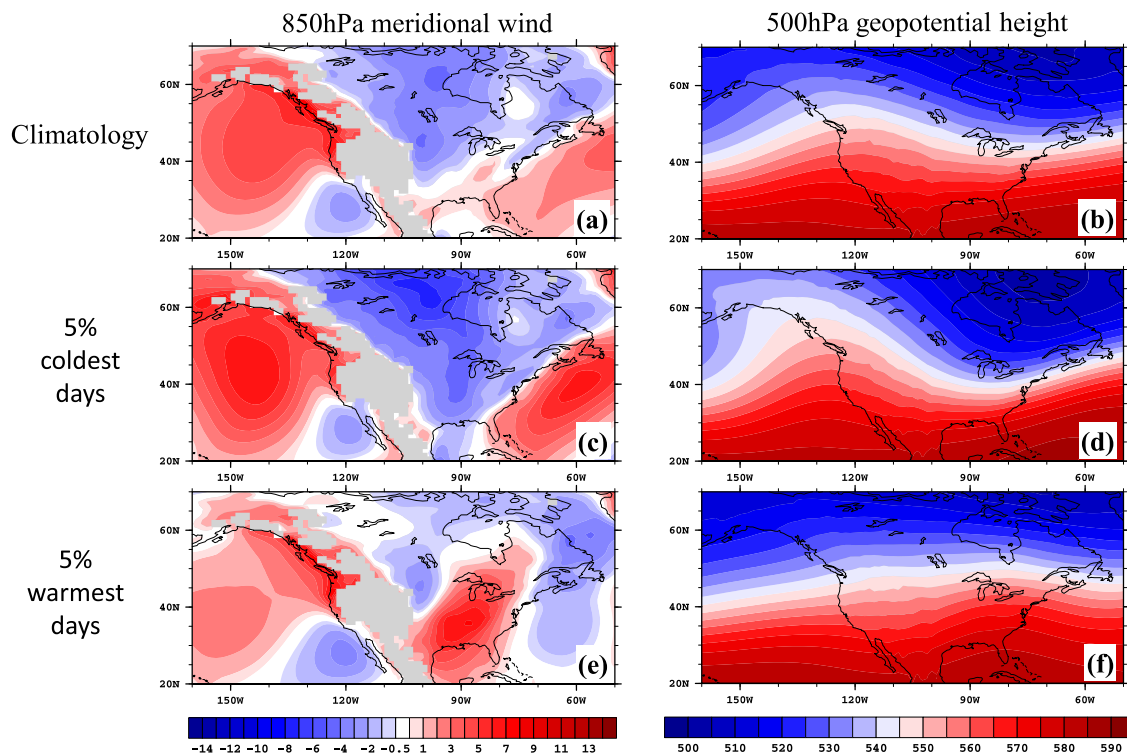


Fig. 9 Spatial pattern of 850 hPa meridional wind (a, c, e) and 500 hPa geopotential height (b, d, f) of climatology (a, b), 5% coldest days (c, d), and 5% warmest days (e, f) during the late twentieth cen-

ture (1971–2000) in CESM-LE. Area higher than 1500 m is masked in 850 hPa Meridional wind field

6 Discussion and conclusions

This study builds on previous work investigating future changes during wintertime over North America and the associated influence of Arctic Amplification on mean and extreme conditions. Our analysis of thermal advection over the continent east of the Rockies enables a more quantitative assessment of the synoptic-scale physical processes than many previous studies on this topic. We have identified several findings that enrich our understanding of North American winter climate in the present and future, including multiple competing mechanisms and the importance of zonal temperature advection.

- CESM realistically simulates the patterns and magnitudes of both zonal and meridional temperature advection during winter in the contemporary climate (Fig. 1). The total thermal advection in both directions is dictated mainly by the “pure climatology term” (i.e., advection by the mean wind across the climatological temperature gradient) (Fig. 2).
- Our study quantifies competing influences on changing temperatures involving meridional versus zonal thermal advection. On average, zonal advection warms the land in the CUS more than meridional advection cools this

region in the present-day (and future) climate (Fig. 2a, b). The projected weakening of both terms suggests that the future mean winter climate over central North America will be affected not only by the well-known upstream warming influence from AA but also by the less-recognized and opposing reduction in zonal heat transport from air masses originating over the Pacific Ocean and adiabatically warmed by the Rockies (Fig. 4a, b). In fact, over most of interior North America, the simulated future cooling influence from weakened zonal advection slightly exceeds the warming effect caused by a reduction in meridional cold-air advection (Fig. 4c). The changes in both types of advection are primarily caused by a slackened horizontal temperature gradient (Figs. 3h, j, 4g, h) and secondarily by a weaker wind speed (Figs. 3d, f, 4d, e).

- Our study also addresses another possible influence on future mean temperature changes: the competition between upstream warming of Arctic air masses versus a more meridional circulation hypothesized to accompany AA, which could enhance the climatological northerly or southerly winds aloft over most of eastern North America. Interestingly, CESM does not produce stronger northerly flow in the mean future climate over most of the continent and, in fact, simulates a southerly wind

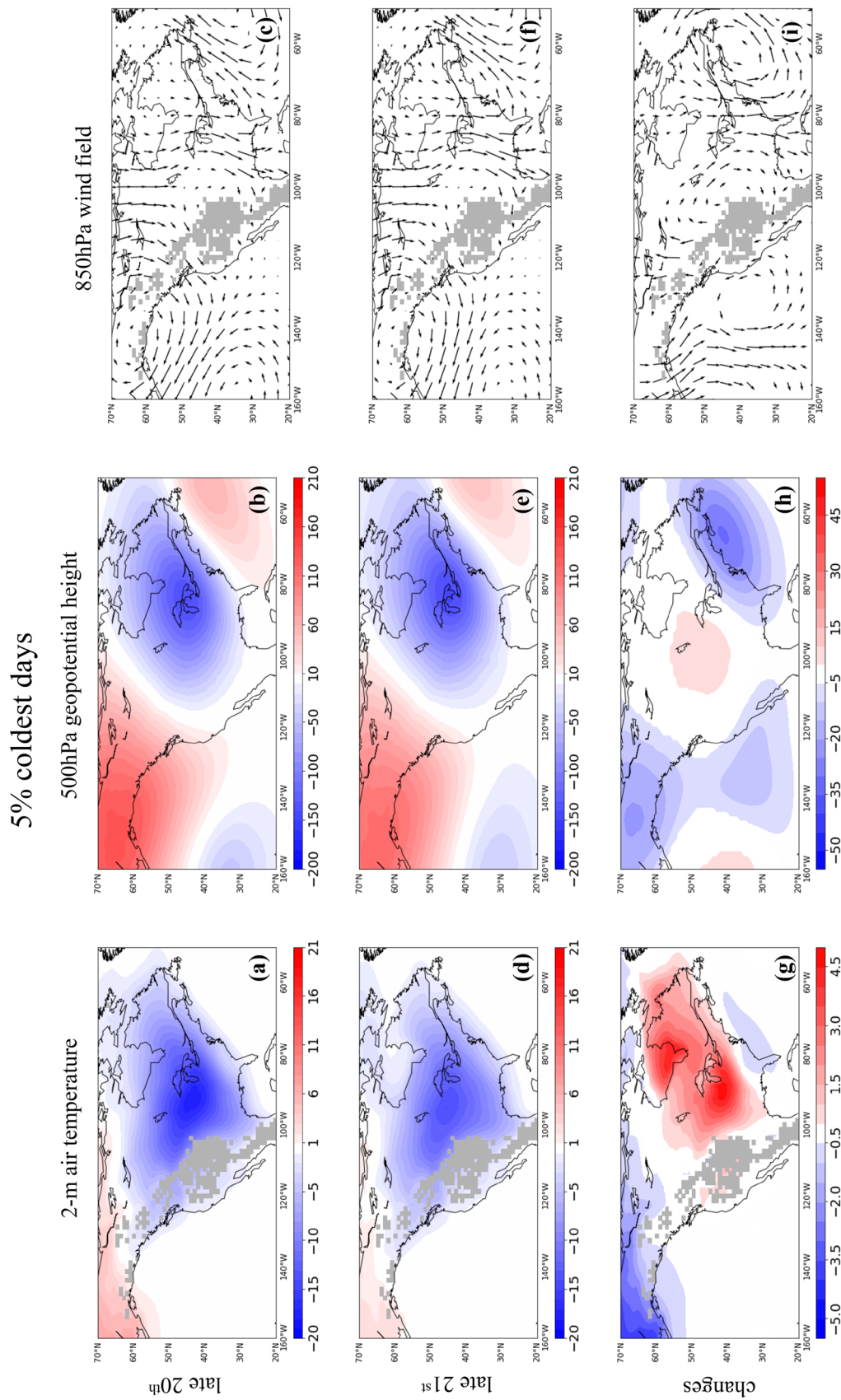


Fig. 10 Anomalous 2-m air temperature (**a, d, g**), 500 hPa geopotential height (**b, e, h**), and 850 hPa wind field (**c, f, i**) during the late twentieth century (**a–c**) and late twenty-first century (**d–f**) and their future changes (**g–i**) on the coldest 5% of winter days in CESM-LE. Area higher than 1500 m is masked. For the future changes, only differences which are significant at the 95% confidence level from a Student’s t-test are shown. For the wind field, if either zonal wind or meridional wind is significant, the wind vector is set as significant

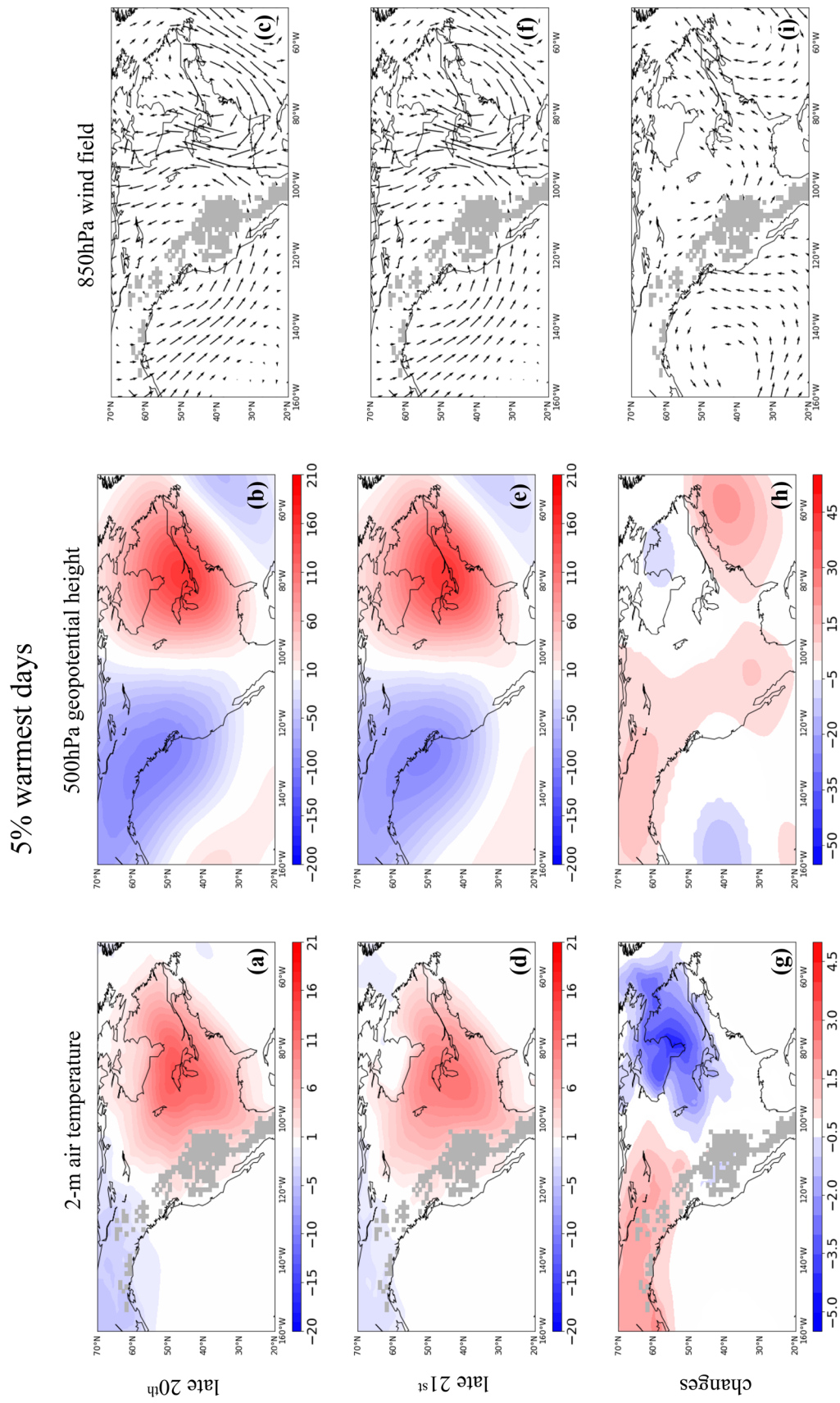


Fig. 11 Same as Fig. 10 but for the 5% warmest days

Future changes on 5% coldest days

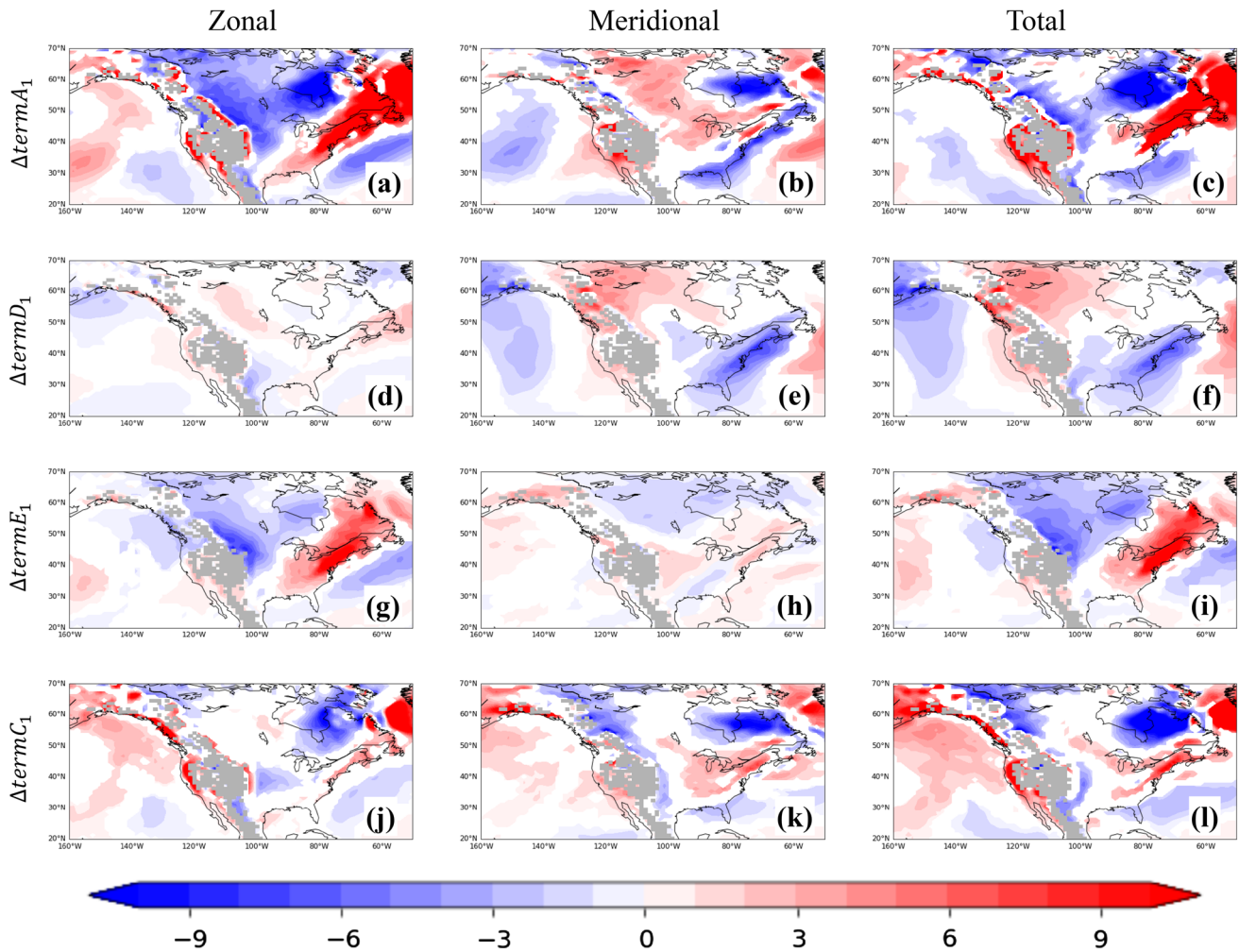


Fig. 12 Future changes (1971–2000 vs 2071–2100) in temperature advection and its components on extreme CUS wintertime cold days in CESM-LE. (unit: K/year). Zonal (a, d, g, j), meridional (b, e, h, k), and total (c, f, i, l) temperature advection. TermA (a–c) and its

components: dynamic term (d–f), thermodynamic term (g–i), and nonlinear term (j–l). Area higher than 1500 m is masked. Only differences which are significant at the 95% confidence level from a Student's t-test are shown

anomaly in an elongated swath to the east of the Rocky Mountains (Fig. 3f). As a consequence, the total mean meridional advection change is dominated by upstream Arctic warming and is strongly positive across most of Canada and much of the northern US and Appalachians, while generally being weakly negative over the southern US (Fig. 4b).

- On extreme winter days over the CUS, the role of thermal advection differs somewhat from the average conditions described above and also differs between very cold and very warm days. During extreme cold events affecting the midsection of the US, meridional cold-air advection dominates most of the continent and reaches far southward to the Gulf of Mexico (Fig. 7b), while

zonal warm-air advection covers much of the interior of North America (Fig. 7a). Unlike the general changes described above, the enhanced cold-air advection on very cold days is driven primarily by the meridional dynamic term (stronger northerly winds; Fig. 7d) and secondarily by the nonlinear term (Fig. 7h), which is largely responsible for the far southern extent of the negative temperature advection anomalies. The nonlinear term is also important for zonal thermal advection, which serves as a substantial mitigating influence by warming the US midsection on extremely cold days (Fig. 7g). By contrast, on extremely warm winter days, both zonal and meridional components produce warm-air advection over most of the US midsection (Fig. 8a, b), primarily due to the

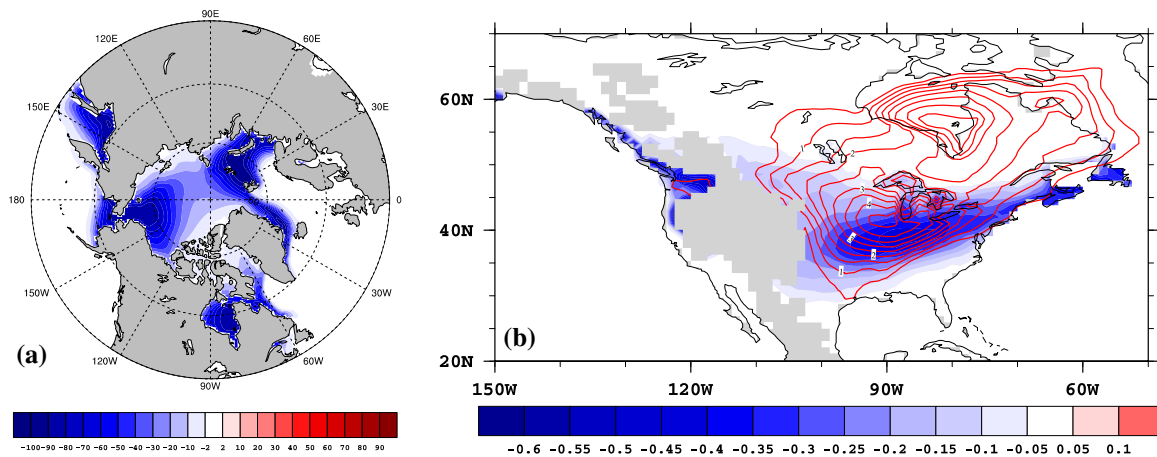


Fig. 13 Changes in **a** sea ice fraction and **b** snow cover fraction (shading) and 2-m air temperature anomaly (contour, interval is 0.5 K) between the future and historical periods on extreme cold

days. Area higher than 1500 m is masked in **b**. Only differences which are significant at the 95% confidence level from a Student's *t*-test are shown

heating effect of southerly winds (Fig. 8d) that are partially offset by cooling from the nonlinear term (Fig. 8h).

- Extreme cold in the future over the CUS is projected to become less severe than in the recent climate, even relative to the higher mean future temperature (Fig. 10g), despite a stronger northerly flow on the coldest days (Fig. 10i) that generates greater cold-air advection (Fig. 12e). A likely explanation for this paradox is the reduction in sea ice and snow cover in the future (Fig. 13) associated with AA. Warmer arctic air masses counter the enhanced advective cooling and appear to weaken the anomalous trough in eastern North America that is representative of the extreme cold (Fig. 10h). This interplay constitutes yet another tug-of-war involving dynamical changes that favor even colder conditions during future CAOs versus surface-based, upwind thermodynamic changes that are responsible for less extreme cold. On the warmest winter days in the future, when snow cover changes play less of a role, the relative (to each 30-year climatology) temperature anomalies in the CUS do not differ much from those in the recent climate, and the circulation differences are also less pronounced than on the coldest days (Fig. 11). The impact on future CAOs from dynamical changes related to thermal advection versus surface-based changes, such as snow cover and sea ice, is a topic ripe for further research.

Acknowledgements This work was supported by NSF grants PLR-1304398 and PLR-1304097. Computing resources on NCAR's Yellowstone and Cheyenne supercomputers were provided by the Computational and Information Systems Laboratory, sponsored by the National Science Foundation.

References

- Ayarzagüena B, Screen JA (2016) Future Arctic sea ice loss reduces severity of cold air outbreaks in midlatitudes. *Geophys Res Lett* 43:2801–2809
- Barnes E (2013) Revisiting the evidence linking Arctic amplification to extreme weather in midlatitudes. *Geophys Res Lett* 40:4734–4739
- Barnes E, Polvani LM (2015) CMIP5 projections of Arctic amplification, of the North American/North Atlantic circulation, and of their relationship. *J Clim* 28:5254–5271
- Barnes E, Dunn-Sigouin E, Masato G, Woolings T (2014) Exploring recent trends in Northern Hemisphere blocking. *Geophys Res Lett* 41:638–644
- Brinkmann WAR (1974) Strong downslope winds at Boulder, Colorado. *Mon Weather Rev* 102:592–602
- Cellitti PM, Walsh JE, Rauber RM, Portis DH (2006) Extreme cold air outbreaks over the United States, the polar vortex, and the large-scale circulation. *J Geophys Res* 111:D02114
- Cohen J (2016) An observational analysis: tropical relative to Arctic influence on midlatitude weather in the era of Arctic amplification. *Geophys Res Lett* 43:5287–5294. <https://doi.org/10.1002/2016GL069102>
- Cohen J, Screen J, Furtado JC, Barlow M, Whittleston D, Coumou D, Francis J, Dethloff K, Entekhabi D, Overland J, Jones J (2014) Recent Arctic amplification and extreme mid-latitude weather. *Nat Geosci* 7:627–637
- Cohen J, Pfeiffer K, Francis JA (2018) Warm Arctic episodes linked with increased frequency of extreme winter weather in the United States. *Nat Commun* 9:869
- de Vries H, Haarsma RJ, Hazeleger W (2012) Western European cold spells in current and future climate. *Geophys Res Lett* 39:L04706. <https://doi.org/10.1029/2011GL050665>
- Dee DP, Uppala SM, Simmons AJ, Berrisford P, Poli P, Kobayashi S, Andrae U, Balmaseda MA, Balsamo G, Bauer P, Bechtold P, Beljaars ACM, van de Berg L, Bidlot J, Bormann N, Delsol C, Dragani R, Fuentes M, Geer AJ, Haimberger L, Healy SB, Hersbach H, Hólm EV, Isaksen L, Kållberg P, Köhler M, Matricardi M, McNally AP, Monge-Sanz BM, Morcrette J-J, Park B-K, Peubey C, de Rosnay P, Tavolato C, Thépaut J-N, Vitart F (2011) The

- ERA-Interim reanalysis: configuration and performance of the data assimilation system. *QJR Meteorol Soc* 137:553–597
- Feldstein SB, Lee S (2014) Intraseasonal and interdecadal jet shifts in the Northern Hemisphere: the role of warm pool tropical convection and sea ice. *J Clim* 27:6497–6518
- Francis JA (2017) Why are Arctic linkages to extreme weather still up in the air? *Bull Am Meteorol Soc* 98:2551–2557
- Francis JA, Vavrus SJ (2012) Evidence linking Arctic amplification to extreme weather in mid-latitudes. *Geophys Res Lett* 39:L06801
- Francis JA, Vavrus SJ (2015) Evidence for a wavier jet stream in response to rapid Arctic warming. *Environ Res Lett* 10:2. <https://doi.org/10.1088/1748-9326/10/1/014005>
- Fu Q, Manabe S, Johanson CM (2011) On the warming in the tropical upper troposphere: models versus observations. *Geophys Res Lett* 38:L15704
- Gao Y, Leung LR, Lu J, Masato G (2015) Persistent cold air outbreaks over North America in a warming climate. *Environ Res Lett* 10:044001
- Hartmann DL (2015) Pacific sea surface temperature and the winter of 2014. *Geophys Res Lett* 42:1894–1902
- Hochheim KP, Barber DG (2014) An update on the ice climatology of the Hudson Bay system. *Arct Antarct Alp Res* 46:66–83
- Holmes CR, Woollings T, Hawkins E, de Vries H (2016) Robust future changes in temperature variability under greenhouse gas forcing and the relationship with thermal advection. *J Clim* 29:2221–2236
- Honda M, Inoue J, Yamane S (2009) Influence of low Arctic sea-ice minima on anomalously cold Eurasian winters. *Geophys Res Lett* 36:L08707
- Kay JE, Deser C, Phillips A, Mai A, Hannay C, Strand G, Arblaster J, Bates S, Danabasoglu G, Edwards J, Holland M, Kushner P, Lamarque J-F, Lawrence D, Lindsay K, Middleton A, Munoz E, Neale R, Oleson K, Polvani L, Vertenstein M (2015) The community earth system model (CESM) large ensemble project: a community resource for studying climate change in the presence of internal climate variability. *Bull Am Meteorol Soc* 96:1333–1349. <https://doi.org/10.1175/BAMS-D-13-00255.1>
- Lee M-Y, Hong C-C, Hsu H-H (2015) Compounding effects of warm sea surface temperature and reduced sea ice on the extreme circulation over the extratropical North Pacific and North America during the 2013–2014 boreal winter. *Geophys Res Lett* 42:1612–1618. <https://doi.org/10.1002/2014GL062956>
- Liu J, Curry JA, Wang H, Song M, Horton RM (2012) Impact of declining Arctic sea ice on winter snowfall. *PNAS* 109:4074–4079
- Marinero A, Hilberg S, Changnon D, Angel JR (2015) The North Pacific-driven severe Midwest winter of 2013/14. *J Appl Meteorol Climatol* 54:2141–2151. <https://doi.org/10.1175/JAMC-D-15-0084.1>
- Petoukhov V, Semenov VA (2010) A link between reduced Barents-Kara sea ice and cold winter extremes over the northern continents. *J Geophys Res* 115:D21111
- Polgar CA, Primack RB (2011) Leaf-out phenology of temperate woody plants: from trees to ecosystems. *N Phytol* 191(4):926–941
- Screen JA (2014) Arctic amplification decreases temperature variance in northern mid- to high-latitudes. *Nat Clim Change* 4:577–582
- Screen JA (2017a) The missing Northern European winter cooling response to Arctic sea ice loss. *Nat Commun* 8:14603
- Screen JA (2017b) Far-flung effects of Arctic warming. *Nat Geosci* 10:253–254
- Screen JA, Simmonds I (2013) Exploring links between Arctic amplification and mid-latitude weather. *Geophys Res Lett* 40:959–964
- Screen JA, Deser C, Sun L (2015) Reduced risk of North American cold extremes due to continued Arctic sea ice loss. *Bull Am Meteorol Soc* 96:1489–1503
- Seidel DJ, Free M, Wang JS (2012) Reexamining the warming in the tropical upper troposphere: models versus radiosonde observations. *Geophys Res Lett* 39:L22701. <https://doi.org/10.1029/2012GL053850>
- Serreze MC, Barrett AP, Stroeve JC, Kindig DN, Holland MM (2009) The emergence of surface-based Arctic amplification. *Cryosphere* 3:11–19
- Smith ET, Sheridan SC (2018) The characteristics of extreme cold events and cold air outbreaks in the eastern United States. *Int J Climatol* 38:e807–e820. <https://doi.org/10.1002/joc.5408>
- Sohn B-J, Lee S, Chung E-S, Song H-J (2016) The role of the dry static stability for the recent change in the Pacific Walker Circulation. *J Clim* 29:2765–2779
- Szeto KK (2008) On the extreme variability and change of cold-season temperatures in Northwest Canada. *J Clim* 21:94–113
- Tang Q, Zhang X, Yang X, Francis J (2013) Cold winter extremes in northern continents linked to Arctic sea ice loss. *Environ Res Lett* 8:014036
- Vaughan DG, Comiso J, Allison I, Carrasco J, Kaser G, Kwok R et al (2013) Observations: cryosphere. In: Stocker TF, Qin D, Plattner GK, Tignor M, Allen SK, Boschung J, Nauels A et al (eds) *Climate change 2013: the physical science basis. Contribution of working group I to the fifth assessment report of the intergovernmental panel on climate change*. Cambridge University Press, Cambridge
- Vavrus S (2007) The role of terrestrial snow cover in the climate system. *Clim Dyn* 29:73–88
- Vavrus SJ, Wang F, Martin JE, Francis JA, Peings Y, Cattiaux J (2017) Changes in North American atmospheric circulation and extreme weather: influence of Arctic amplification and northern hemisphere snow cover. *J Clim* 30:4317–4333
- Wallace JM, Held IM, Thompson D, Trenberth KE, Walsh JE (2014) Global warming and winter weather. *Science* 343:729–730
- Walsh JE, Phillips AS, Portis DH, Chapman WL (2001) Extreme cold outbreaks in the United States and Europe, 1948–99. *J Clim* 14:2642–2658
- Wang C, Liu H, Lee S-K (2010) The record-breaking cold temperatures during the winter of 2009/2010 in the Northern Hemisphere. *Atmos Sci Lett* 11:161–168

Publisher's Note Springer Nature remains neutral with regard to jurisdictional claims in published maps and institutional affiliations.